HNUE JOURNAL OF SCIENCE
Natural Sciences 2024, Volume 69, Issue 1, pp. 51-66
This paper is available online at http://stdb.hnue.edu.vn
DOI: 10.18173/2354-1059.2024-0005

STUDY ON THERMODYNAMIC PROPERTY OF THIN FILM OF BCC INTERSTITIAL ALLOY WSi AT ZERO PRESSURE: DEPENDENCE ON TEMPERATURE, INTERSTITIAL ATOM CONCENTRATION AND FILM THICKNESS

Dương Dai Phuong[1], Nguyen Quang Hoc[2,*], Hua Xuan Dat[3],
Pham Phuong Uyen[4] and Doan Manh Hung[5]
[1]Tank Armour Officers Training School, Tam Duong, Vinh Phuc province, Vietnam
[2]Faculty of Physics, Hanoi National University of Education, Hanoi city, Vietnam
[*]Corresponding author: Nguyen Quang Hoc, e-mail: hocnq@hnue.edu.vn

Received December 8, 2023. Revised March 20, 2024. Accepted March 27, 2024.

Abstract. The article presents a model and derives analytical expressions for Helmholtz free energy, the nearest neighbor distance, isothermal compressibility, the thermal expansion coefficient, the heat capacities at constant volume and constant pressure as functions of temperature, concentration of interstitial atoms, and film's thickness for an interstitial binary alloy with a BCC structure based on the statistical moment method (SMM). The theoretical results are applied to numerical calculations for films of W and WSi. The temperature and interstitial atom concentration dependences of thermodynamic quantities for the alloy WSi's film are similar to those for the metal W film. When the film thickness increases to about 40 nm, the thermodynamic properties of the film approach those of the bulk material. The SMM numerical results for W agree well with experimental data and other calculation results. Other SMM numerical results are new and predict future experimental results.

Keywords: WSi, interstitial alloy, film's thickness, thermodynamic property, SMM.

1. Introduction

Research on thin film materials has developed strongly in recent years because thin films have interesting properties different from bulk materials such as durability, lightness, abrasion resistance, and high pressure resistance. They are widely used in many fields of science and technology and are tools in the military, medical, electronic equipment, etc, [1]-[5]. The properties of thin films depend on many factors such as system structure, size, temperature, pressure, and interstitial particle concentration [6]-[9]. The thermal expansion coefficient of a thin film mounted on a substrate depends on temperature [10], [11]. The thermal expansion coefficient of the interstitial alloy's thin film depends on film thickness. For an FCC interstitial alloy's thin film, the thermal expansion coefficient increases with thickness, and for a BCC interstitial alloy's thin film, the thermal expansion coefficient decreases with increasing thickness [12].

Some mechanical and thermodynamic properties of interstitial alloy thin films have been studied in [13]. Thermodynamic properties of the interstitial alloy and metal thin films with the FCC structure have been studied using the statistical model method (SMM) in order to take into account the anharmonic contribution of lattice vibrations [14]. Thermodynamic quantities of thin films depend on temperature, pressure, interstitial particle concentration, and film thickness. Most studies on the dependence of thermodynamic quantities of interstitial alloy thin films on structure, size, and temperature have not been studied in detail. Moreover, the studies are mainly in the low temperature range and at zero pressure. SMM has been applied to study the thermodynamic, elastic, and diffusion properties of metals and alloys [15]-[21], and thermodynamic and elastic properties of thin films of metal thin films [22]-[25]. However, an SMM study on the thermodynamic properties of BCC interstitial alloy thin films still is an open problem

In this work, for the first time, we give the thermodynamic theory depending on temperature, interstitial atom concentration, and film thickness for the BCC interstitial binary alloy's film based on SMM. The theoretical results are applied to numerical calculations for films of W and WSi.

2. Content

Assume a free thin film of BCC interstitial alloy AB has n^* layers with the thickness d. This film consists of two outer layers with the number of atoms N_n, two neighboring outer layers with the number of atoms N_{sn}, and n^*- 4 inner layers with the number of atoms N_t.

The cohesive energy, u_0 and the crystal parameters, k, γ_1, γ_2, γ for interstitial atoms B at the face center of the cubic unit cell in the approximation of two coordination spheres, for atoms A termed A_1 at the body center of the cubic unit cell, and for atoms A termed A_2 at the vertices of the cubic unit cell (in the approximation of three coordination spheres for the inner layers t, the next outer layers sn (where there is a particle vacancy on the z axis in the second coordination sphere), and the outer layers n (remove an atom on the 2nd coordination sphere when calculating the cohesive energy and crystal parameters of atom B and remove an atom on the 3rd coordination sphere when calculating the cohesive energy and crystal parameters of atoms A_1 and A_2) of BCC interstitial alloy AB's thin film respectively have the form [14], [21]

$$u_{0B}^t = \frac{1}{2}\sum_{i=1}^{n_i}\varphi_{AB}^t(r_i) = \varphi_{AB}^t\left(r_{1B}^t\right) + 2\varphi_{AB}^t\left(r_{2B}^t\right), r_{2B}^t = \sqrt{2}r_{1B}^t, \tag{1}$$

$$k_B^t = \frac{1}{2}\sum_i\left(\frac{\partial^2\varphi_{AB}^t}{\partial u_{i\beta}^{t2}}\right)_{eq} = \frac{1}{r_{1B}^t}\frac{d\varphi_{AB}^t\left(r_{1B}^t\right)}{dr_{1B}^t} + \frac{d^2\varphi_{AB}^t\left(r_{2B}^t\right)}{dr_{2B}^{t2}} + \frac{1}{r_{2B}^t}\frac{d\varphi_{AB}^t\left(r_{2B}^t\right)}{dr_{2B}^t}, \tag{2}$$

$$\gamma_{1B}^{t}=\frac{1}{48}\sum_{i}\left(\frac{\partial^{4}\varphi_{AB}^{t}}{\partial u_{i\beta}^{t4}}\right)_{eq}=\frac{1}{8r_{1B}^{t2}}\frac{d^{2}\varphi_{AB}^{t}(r_{1B}^{t})}{dr_{1B}^{t2}}-\frac{1}{8r_{1B}^{t3}}\frac{d\varphi_{AB}^{t}(r_{1B}^{t})}{dr_{1B}^{t}}+\frac{1}{48}\frac{d^{4}\varphi_{AB}^{t}(r_{2B}^{t})}{dr_{2B}^{t4}}+$$

$$+\frac{1}{8r_{2B}^{t}}\frac{d^{3}\varphi_{AB}^{t}(r_{2B}^{t})}{dr_{2B}^{t3}}-\frac{3}{16r_{2B}^{t2}}\frac{d^{2}\varphi_{AB}^{t}(r_{2B}^{t})}{dr_{2B}^{t2}}+\frac{3}{16r_{2B}^{t3}}\frac{d\varphi_{AB}^{t}(r_{2B}^{t})}{dr_{2B}^{t}},\tag{3}$$

$$\gamma_{2B}^{t}=\frac{6}{48}\sum_{i}\left(\frac{\partial^{4}\varphi_{AB}^{t}}{\partial u_{i\alpha}^{t2}\partial u_{i\beta}^{t2}}\right)_{eq}=\frac{1}{4r_{1B}^{t}}\frac{d^{3}\varphi_{AB}^{t}(r_{1B}^{t})}{dr_{1B}^{t3}}-\frac{1}{2r_{1B}^{t2}}\frac{d^{2}\varphi_{AB}^{t}(r_{1B}^{t})}{dr_{1B}^{t2}}+\frac{1}{2r_{1B}^{t3}}\frac{d\varphi_{AB}^{t}(r_{1B}^{t})}{dr_{1B}^{t}}+$$

$$+\frac{1}{4r_{2B}^{t}}\frac{d^{3}\varphi_{AB}^{t}(r_{2B}^{t})}{dr_{2B}^{t3}}-\frac{1}{4r_{2B}^{t2}}\frac{d^{2}\varphi_{AB}^{t}(r_{2B}^{t})}{dr_{2B}^{t2}}+\frac{1}{4r_{2B}^{t3}}\frac{d\varphi_{AB}^{t}(r_{2B}^{t})}{dr_{2B}^{t}},\tag{4}$$

$$u_{0A_1}^{t}=u_{0A}^{t}+3\varphi_{A_1B}^{t}\left(r_{1A_1}^{t}\right),\tag{5}$$

$$k_{A_1}^{t}=k_{A}^{t}+\frac{1}{2}\sum_{i}\left[\left(\frac{\partial^{2}\varphi_{A_1B}^{t}}{\partial u_{i\beta}^{t2}}\right)_{eq}\right]_{r=r_{1A_1}}=k_{A}^{t}+\frac{d^{2}\varphi_{A_1B}^{t}\left(r_{1A_1}^{t}\right)}{dr_{1A_1}^{t2}}+\frac{2}{r_{1A_1}^{t}}\frac{d\varphi_{A_1B}^{t}\left(r_{1A_1}^{t}\right)}{dr_{1A_1}^{t}},\tag{6}$$

$$\gamma_{1A_1}^{t}=\gamma_{1A}^{t}+\frac{1}{48}\sum_{i}\left[\left(\frac{\partial^{4}\varphi_{A_1B}^{t}}{\partial u_{i\beta}^{t4}}\right)_{eq}\right]_{r=r_{1A_1}}=$$

$$=\gamma_{1A}^{t}+\frac{1}{24}\frac{d^{4}\varphi_{A_1B}^{t}\left(r_{1A_1}^{t}\right)}{dr_{1A_1}^{t4}}-\frac{1}{6r_{1A_1}^{t}}\frac{d^{3}\varphi_{A_1B}^{t}\left(r_{1A_1}^{t}\right)}{dr_{1A_1}^{t3}}+\frac{3}{4r_{1A_1}^{t2}}\frac{d^{2}\varphi_{A_1B}^{t}\left(r_{1A_1}^{t}\right)}{dr_{1A_1}^{t2}}-\frac{3}{4r_{1A_1}^{t3}}\frac{d\varphi_{A_1B}^{t}\left(r_{1A_1}^{t}\right)}{dr_{1A_1}^{t}},\tag{7}$$

$$\gamma_{2A_1}^{t}=\gamma_{2A}^{t}+\frac{6}{48}\sum_{i}\left[\left(\frac{\partial^{4}\varphi_{A_1B}^{t}}{\partial u_{i\alpha}^{t2}\partial u_{i\beta}^{t2}}\right)_{eq}\right]_{r=r_{1A_1}}=\gamma_{2A}^{t}+\frac{1}{4r_{1A_1}^{t}}\frac{d^{3}\varphi_{A_1B}^{t}(r_{1A_1}^{t})}{dr_{1A_1}^{t3}},\tag{8}$$

$$u_{0A_2}^{t}=u_{0A}^{t}+6\varphi_{A_2B}^{t}\left(r_{1A_2}^{t}\right),\tag{9}$$

$$k_{A_2}^{t}=k_{A}^{t}+\frac{1}{2}\sum_{i}\left[\left(\frac{\partial^{2}\varphi_{A_2B}^{t}}{\partial u_{i\beta}^{t2}}\right)_{eq}\right]_{r=r_{1A_2}}=k_{A}^{t}+2\frac{d^{2}\varphi_{A_2B}^{t}\left(r_{1A_2}^{t}\right)}{dr_{1A_2}^{t2}}+\frac{4}{r_{1A_2}^{t}}\frac{d\varphi_{A_2B}^{t}\left(r_{1A_2}^{t}\right)}{dr_{1A_2}^{t}},\tag{10}$$

$$\gamma_{1A_2}^{t}=\gamma_{1A}^{t}+\frac{1}{48}\sum_{i}\left[\left(\frac{\partial^{4}\varphi_{A_2B}^{t}}{\partial u_{i\beta}^{t4}}\right)_{eq}\right]_{r=r_{1A_2}}=\gamma_{1A}^{t}+\frac{1}{24}\frac{d^{4}\varphi_{A_2B}^{t}(r_{1A_2}^{t})}{dr_{1A_2}^{t4}}+\frac{5}{12r_{1A_2}^{t}}\frac{d^{3}\varphi_{A_2B}^{t}(r_{1A_2}^{t})}{dr_{1A_2}^{t3}}+$$

$$-\frac{1}{8r_{1A_2}^{t2}}\frac{d^{2}\varphi_{A_2B}^{t}(r_{1A_2}^{t})}{dr_{1A_2}^{t2}}+\frac{1}{8r_{1A_2}^{t3}}\frac{d\varphi_{A_2B}^{t}(r_{1A_2}^{t})}{dr_{1A_2}^{t}},\tag{11}$$

$$\gamma_{2A_2}^{t}=\gamma_{2A}^{t}+\frac{6}{48}\sum_{i}\left[\left(\frac{\partial^{4}\varphi_{A_2B}^{t}}{\partial u_{i\alpha}^{t2}\partial u_{i\beta}^{t2}}\right)_{eq}\right]_{r=r_{1A_2}}=\gamma_{2A}^{t}+\frac{1}{8}\frac{d^{4}\varphi_{A_2B}^{t}(r_{1A_2}^{t})}{dr_{1A_2}^{t4}}+$$

$$+\frac{1}{4r_{1A_2}^{t}}\frac{d^{3}\varphi_{A_2B}^{t}(r_{1A_2}^{t})}{dr_{1A_2}^{t3}}+\frac{3}{8r_{1A_2}^{t2}}\frac{d^{2}\varphi_{A_2B}^{t}(r_{1A_2}^{t})}{dr_{1A_2}^{t2}}-\frac{3}{8r_{1A_2}^{t3}}\frac{d\varphi_{A_2B}^{t}(r_{1A_2}^{t})}{dr_{1A_2}^{t}},\tag{12}$$

$$u_{0A}^{t} = 4\varphi_{AA}^{t}\left(r_{1A}^{t}\right) + 3\varphi_{AA}^{t}\left(r_{2A}^{t}\right),\ r_{2A}^{t} = \frac{2}{\sqrt{3}}r_{1A}^{t}, \tag{13}$$

$$k_{A}^{t} = \frac{4}{3}\frac{d^{2}\varphi_{AA}^{t}\left(r_{1A}^{t}\right)}{dr_{1A}^{t2}} + \frac{8}{3r_{1A}^{t}}\frac{d\varphi_{AA}^{t}\left(r_{1A}^{t}\right)}{dr_{1A}^{t}} + \frac{d^{2}\varphi_{AA}^{t}\left(r_{2A}^{t}\right)}{dr_{2A}^{t2}} + \frac{2}{r_{2A}^{t}}\frac{d\varphi_{AA}^{t}\left(r_{2A}^{t}\right)}{dr_{2A}^{t}}, \tag{14}$$

$$\gamma_{1A}^{t} = \frac{1}{54}\frac{d^{4}\varphi_{AA}^{t}\left(r_{1A}^{t}\right)}{dr_{1A}^{t4}} + \frac{2}{9r_{1A}^{t}}\frac{d^{3}\varphi_{AA}^{t}\left(r_{1A}^{t}\right)}{dr_{1A}^{t3}} - \frac{2}{9r_{1A}^{t2}}\frac{d^{2}\varphi_{AA}^{t}\left(r_{1A}^{t}\right)}{dr_{1A}^{t2}} + \frac{2}{9r_{1A}^{t3}}\frac{d\varphi_{AA}^{t}\left(r_{1A}^{t}\right)}{dr_{1A}^{t}} +$$

$$+\frac{1}{24}\frac{d^{4}\varphi_{AA}^{t}\left(r_{2A}^{t}\right)}{dr_{2A}^{t4}} + \frac{1}{4r_{2A}^{t2}}\frac{d^{2}\varphi_{AA}^{t}\left(r_{2A}^{t}\right)}{dr_{2A}^{t2}} - \frac{1}{4r_{2A}^{t3}}\frac{d\varphi_{AA}^{t}\left(r_{2A}^{t}\right)}{dr_{2A}^{t}}, \tag{15}$$

$$\gamma_{2A}^{t} = \frac{1}{9}\frac{d^{4}\varphi_{AA}^{t}\left(r_{1A}^{t}\right)}{dr_{1A}^{t4}} + \frac{2}{3r_{1A}^{t2}}\frac{d^{2}\varphi_{AA}^{t}\left(r_{1A}^{t}\right)}{dr_{1A}^{t2}} - \frac{2}{3r_{1A}^{t3}}\frac{d\varphi_{AA}^{t}\left(r_{1A}^{t}\right)}{dr_{1A}^{t}} + \frac{1}{2r_{2A}^{t}}\frac{d^{3}\varphi_{AA}^{t}\left(r_{2A}^{t}\right)}{dr_{2A}^{t3}}, \tag{16}$$

$$u_{0B}^{sn} = \frac{1}{2}\sum_{i=1}^{n_i}\varphi_{AB}^{sn}(r_i) = \varphi_{AB}^{sn}\left(r_{1B}^{sn}\right) + 2\varphi_{AB}^{sn}\left(r_{2B}^{sn}\right),\ r_{2B}^{sn} = \sqrt{2}r_{1B}^{sn}, \tag{17}$$

$$k_{B}^{sn} = \frac{1}{2}\sum_{i}\left(\frac{\partial^{2}\varphi_{AB}^{sn}}{\partial u_{i\beta}^{sn2}}\right)_{eq} = \frac{1}{r_{1B}^{n1}}\frac{d\varphi_{AB}^{sn}\left(r_{1B}^{sn}\right)}{dr_{1B}^{sn}} + \frac{d^{2}\varphi_{AB}^{sn}\left(r_{2B}^{sn}\right)}{dr_{2B}^{sn2}} + \frac{1}{r_{2B}^{sn}}\frac{d\varphi_{AB}^{sn}\left(r_{2B}^{sn}\right)}{dr_{2B}^{sn}}, \tag{18}$$

$$\gamma_{1B}^{sn} = \frac{1}{48}\sum_{i}\left(\frac{\partial^{4}\varphi_{AB}^{sn}}{\partial u_{i\beta}^{sn4}}\right)_{eq} = \frac{1}{8r_{1B}^{sn2}}\frac{d^{2}\varphi_{AB}^{sn}(r_{1B}^{sn})}{dr_{1B}^{sn2}} - \frac{1}{8r_{1B}^{sn3}}\frac{d\varphi_{AB}^{sn}(r_{1B}^{sn})}{dr_{1B}^{sn}} + \frac{1}{48}\frac{d^{4}\varphi_{AB}^{sn}(r_{2B}^{sn})}{dr_{2B}^{sn4}} +$$

$$+\frac{1}{8r_{2B}^{sn}}\frac{d^{3}\varphi_{AB}^{sn}(r_{2B}^{sn})}{dr_{2B}^{sn3}} - \frac{3}{16r_{2B}^{sn2}}\frac{d^{2}\varphi_{AB}^{sn}(r_{2B}^{sn})}{dr_{2B}^{sn2}} + \frac{3}{16r_{2B}^{sn3}}\frac{d\varphi_{AB}^{sn}(r_{2B}^{sn})}{dr_{2B}^{sn}}, \tag{19}$$

$$\gamma_{2B}^{sn} = \frac{6}{48}\sum_{i}\left(\frac{\partial^{4}\varphi_{AB}^{sn}}{\partial u_{i\alpha}^{sn2}\partial u_{i\beta}^{sn2}}\right)_{eq} = \frac{1}{4r_{1B}^{sn}}\frac{d^{3}\varphi_{AB}^{sn}(r_{1B}^{sn})}{dr_{1B}^{sn3}} - \frac{1}{2r_{1B}^{sn2}}\frac{d^{2}\varphi_{AB}^{sn}(r_{1B}^{sn})}{dr_{1B}^{sn2}} + \frac{1}{2r_{1B}^{sn3}}\frac{d\varphi_{AB}^{sn}(r_{1B}^{sn})}{dr_{1B}^{sn}} +$$

$$+\frac{1}{4r_{2B}^{sn}}\frac{d^{3}\varphi_{AB}^{sn}(r_{2B}^{sn})}{dr_{2B}^{sn3}} - \frac{1}{4r_{2B}^{sn2}}\frac{d^{2}\varphi_{AB}^{sn}(r_{2B}^{sn})}{dr_{2B}^{sn2}} + \frac{1}{4r_{2B}^{sn3}}\frac{d\varphi_{AB}^{sn}(r_{2B}^{sn})}{dr_{2B}^{sn}}, \tag{20}$$

$$u_{0A_1}^{sn} = u_{0A}^{sn} + 2\varphi_{A_1B}^{sn}\left(r_{1A_1}^{sn}\right), \tag{21}$$

$$k_{A_1}^{sn} = k_{A}^{sn} + \frac{1}{2}\sum_{i}\left[\left(\frac{\partial^{2}\varphi_{A_1B}^{sn}}{\partial u_{i\beta}^{sn2}}\right)_{eq}\right]_{r=r_{1A_1}} = k_{A}^{sn} + \frac{d^{2}\varphi_{A_1B}^{sn}\left(r_{1A_1}^{sn}\right)}{dr_{1A_1}^{sn2}} + \frac{1}{r_{1A_1}^{sn}}\frac{d\varphi_{A_1B}^{sn}\left(r_{1A_1}^{sn}\right)}{dr_{1A_1}^{sn}}, \tag{22}$$

$$\gamma_{1A_1}^{sn} = \gamma_{1A}^{sn} + \frac{1}{48}\sum_{i}\left[\left(\frac{\partial^{4}\varphi_{A_1B}^{sn}}{\partial u_{i\beta}^{sn4}}\right)_{eq}\right]_{r=r_{1A_1}} =$$

$$= \gamma_{1A}^{sn} + \frac{1}{24}\frac{d^{4}\varphi_{A_1B}^{sn}\left(r_{1A_1}^{sn}\right)}{dr_{1A_1}^{sn4}} - \frac{1}{6r_{1A_1}^{sn}}\frac{d^{3}\varphi_{A_1B}^{sn}\left(r_{1A_1}^{sn}\right)}{dr_{1A_1}^{sn3}} + \frac{5}{8r_{1A_1}^{sn2}}\frac{d^{2}\varphi_{A_1B}^{sn}\left(r_{1A_1}^{sn}\right)}{dr_{1A_1}^{sn2}} - \frac{5}{8r_{1A_1}^{sn3}}\frac{d\varphi_{A_1B}^{sn}\left(r_{1A_1}^{sn}\right)}{dr_{1A_1}^{sn}}, \tag{23}$$

$$\gamma_{2A_1}^{sn} = \gamma_{2A}^{sn} + \frac{6}{48}\sum_{i}\left[\left(\frac{\partial^{4}\varphi_{A_1B}^{sn}}{\partial u_{i\alpha}^{sn2}\partial u_{i\beta}^{sn2}}\right)_{eq}\right]_{r=r_{1A_1}} = \gamma_{2A}^{sn} + \frac{1}{4r_{1A_1}^{sn}}\frac{d^{3}\varphi_{A_1B}^{sn}(r_{1A_1}^{sn})}{dr_{1A_1}^{sn3}} -$$

$$-\frac{1}{4r_{1A_1}^{sn2}}\frac{d^2\varphi_{A_1B}^{sn}(r_{1A_1}^{sn})}{dr_{1A_1}^{sn2}}+\frac{1}{4r_{1A_1}^{sn3}}\frac{d\varphi_{A_1B}^{sn}(r_{1A_1}^{sn})}{dr_{1A_1}^{sn}}, \tag{24}$$

$$u_{0A_2}^{sn}=u_{0A}^{sn}+6\varphi_{A_2B}^{sn}\left(r_{1A_2}^{sn}\right), \tag{25}$$

$$k_{A_2}^{sn}=k_A^{sn}+\frac{1}{2}\sum_i\left[\left(\frac{\partial^2\varphi_{A_2B}^{sn}}{\partial u_{i\beta}^{sn2}}\right)_{eq}\right]_{r=r_{1A_2}}=k_A^{sn}+\ 2\frac{d^2\varphi_{A_2B}^{sn}\left(r_{1A_2}^{sn}\right)}{dr_{1A_2}^{sn2}}+\frac{4}{r_{1A_2}^{sn}}\frac{d\varphi_{A_2B}^{sn}\left(r_{1A_2}^{sn}\right)}{dr_{1A_2}^{sn}}, \tag{26}$$

$$\gamma_{1A_2}^{sn}=\gamma_{1A}^{sn}+\frac{1}{48}\sum_i\left[\left(\frac{\partial^4\varphi_{A_2B}^{sn}}{\partial u_{i\beta}^{sn4}}\right)_{eq}\right]_{r=r_{1A_2}}=\gamma_{1A}^{sn}+\frac{1}{24}\frac{d^4\varphi_{A_2B}^{sn}(r_{1A_2}^{sn})}{dr_{1A_2}^{sn4}}+\frac{5}{12r_{1A_2}^{sn}}\frac{d^3\varphi_{A_2B}^{sn}(r_{1A_2}^{sn})}{dr_{1A_2}^{sn3}}+$$

$$-\frac{1}{8r_{1A_2}^{sn2}}\frac{d^2\varphi_{A_2B}^{sn}(r_{1A_2}^{sn})}{dr_{1A_2}^{sn2}}+\frac{1}{8r_{1A_2}^{sn3}}\frac{d\varphi_{A_2B}^{sn}(r_{1A_2}^{sn})}{dr_{1A_2}^{sn}}, \tag{27}$$

$$\gamma_{2A_2}^{sn}=\gamma_{2A}^{sn}+\frac{6}{48}\sum_i\left[\left(\frac{\partial^4\varphi_{A_2B}^{sn}}{\partial u_{i\alpha}^{sn2}\partial u_{i\beta}^{sn2}}\right)_{eq}\right]_{r=r_{1A_2}}=\gamma_{2A}^{sn}+\frac{1}{8}\frac{d^4\varphi_{A_2B}^{sn}(r_{1A_2}^{sn})}{dr_{1A_2}^{sn4}}+$$

$$+\frac{1}{4r_{1A_2}^{sn}}\frac{d^3\varphi_{A_2B}^{sn}(r_{1A_2}^{sn})}{dr_{1A_2}^{sn3}}+\frac{3}{8r_{1A_2}^{sn2}}\frac{d^2\varphi_{A_2B}^{sn}(r_{1A_2}^{sn})}{dr_{1A_2}^{sn2}}-\frac{3}{8r_{1A_2}^{sn3}}\frac{d\varphi_{A_2B}^{sn}(r_{1A_2}^{sn})}{dr_{1A_2}^{sn}}, \tag{28}$$

$$u_{0A}^{sn}=\ 4\varphi_{AA}^{sn}\left(r_{1A}^{sn}\right)+\ 3\varphi_{AA}^{sn}\left(r_{2A}^{sn}\right),\ r_{2A}^{sn}=\frac{2}{\sqrt{3}}r_{1A}^{sn}, \tag{29}$$

$$k_A^{sn}=\frac{4}{3}\frac{d^2\varphi_{AA}^{sn}\left(r_{1A}^{sn}\right)}{dr_{1A}^{sn2}}+\frac{8}{3r_{1A}^{sn}}\frac{d\varphi_{AA}^{sn}\left(r_{1A}^{sn}\right)}{dr_{1A}^{sn}}+\frac{d^2\varphi_{AA}^{sn}\left(r_{2A}^{sn}\right)}{dr_{2A}^{sn2}}+\frac{2}{r_{2A}^{sn}}\frac{d\varphi_{AA}^{sn}\left(r_{2A}^{sn}\right)}{dr_{2A}^{sn}}, \tag{30}$$

$$\gamma_{1A}^{sn}=\frac{1}{54}\frac{d^4\varphi_{AA}^{sn}\left(r_{1A}^{sn}\right)}{dr_{1A}^{sn4}}+\frac{2}{9r_{1A}^{sn}}\frac{d^3\varphi_{AA}^{sn}\left(r_{1A}^{sn}\right)}{dr_{1A}^{sn3}}-\frac{2}{9r_{1A}^{sn2}}\frac{d^2\varphi_{AA}^{sn}\left(r_{1A}^{sn}\right)}{dr_{1A}^{sn2}}+\frac{2}{9r_{1A}^{sn3}}\frac{d\varphi_{AA}^{sn}\left(r_{1A}^{sn}\right)}{dr_{1A}^{sn}}+$$

$$+\frac{1}{24}\frac{d^4\varphi_{AA}^{sn}\left(r_{2A}^{sn}\right)}{dr_{2A}^{sn4}}+\frac{1}{4r_{2A}^{sn2}}\frac{d^2\varphi_{AA}^{sn}\left(r_{2A}^{sn}\right)}{dr_{2A}^{sn2}}-\frac{1}{4r_{2A}^{sn3}}\frac{d\varphi_{AA}^{sn}\left(r_{2A}^{sn}\right)}{dr_{2A}^{sn}}, \tag{31}$$

$$\gamma_{2A}^{sn}=\frac{1}{9}\frac{d^4\varphi_{AA}^{sn}\left(r_{1A}^{sn}\right)}{dr_{1A}^{sn4}}+\frac{2}{3r_{1A}^{sn2}}\frac{d^2\varphi_{AA}^{sn}\left(r_{1A}^{sn}\right)}{dr_{1A}^{sn2}}-\frac{2}{3r_{1A}^{sn3}}\frac{d\varphi_{AA}^{sn}\left(r_{1A}^{sn}\right)}{dr_{1A}^{sn}}+\frac{1}{2r_{2A}^{sn}}\frac{d^3\varphi_{AA}^{sn}\left(r_{2A}^{sn}\right)}{dr_{2A}^{sn3}}\cdot \tag{32}$$

$$u_{0B}^n=\frac{1}{2}\sum_{i=1}^{n_i}\varphi_{AB}^n(r_i)=\varphi_{AB}^n\left(r_{1B}^n\right)+\ \frac{3}{2}\varphi_{AB}^n\left(r_{2B}^n\right),\ r_{2B}^n=\ \sqrt{2}r_{1B}^n, \tag{33}$$

$$k_B^n=\frac{1}{2}\sum_i\left(\frac{\partial^2\varphi_{AB}^n}{\partial u_{i\beta}^{n2}}\right)_{eq}=\frac{1}{r_{1B}^n}\frac{d\varphi_{AB}^n\left(r_{1B}^n\right)}{dr_{1B}^n}+\frac{3}{4}\frac{d^2\varphi_{AB}^n\left(r_{2B}^n\right)}{dr_{2B}^{n2}}+\frac{3}{4r_{2B}^n}\frac{d\varphi_{AB}^n\left(r_{2B}^n\right)}{dr_{2B}^n}, \tag{34}$$

$$\gamma_{1B}^n=\frac{1}{48}\sum_i\left(\frac{\partial^4\varphi_{AB}^n}{\partial u_{i\beta}^{n4}}\right)_{eq}=\frac{1}{8r_{1B}^{n2}}\frac{d^2\varphi_{AB}^n(r_{1B}^n)}{dr_{1B}^{n2}}-\frac{1}{8r_{1B}^{n3}}\frac{d\varphi_{AB}^n(r_{1B}^n)}{dr_{1B}^n}+\frac{1}{64}\frac{d^4\varphi_{AB}^n(r_{2B}^n)}{dr_{2B}^{n4}}+$$

$$+\frac{3}{32r_{2B}^n}\frac{d^3\varphi_{AB}^n(r_{2B}^n)}{dr_{2B}^{n3}}-\frac{9}{64r_{2B}^{n2}}\frac{d^2\varphi_{AB}^n(r_{2B}^n)}{dr_{2B}^{n2}}+\frac{9}{64r_{2B}^{n3}}\frac{d\varphi_{AB}^n(r_{2B}^n)}{dr_{2B}^n}, \tag{35}$$

$$\gamma_{2B}^{n}=\frac{6}{48}\sum_{i}\left(\frac{\partial^4\varphi_{AB}^{n}}{\partial u_{i\alpha}^{n2}\partial u_{i\beta}^{n2}}\right)_{eq}=\frac{1}{4r_{1B}^{n}}\frac{d^3\varphi_{AB}^{n}(r_{1B}^{n})}{dr_{1B}^{n3}}-\frac{1}{2r_{1B}^{n2}}\frac{d^2\varphi_{AB}^{n}(r_{1B}^{n})}{dr_{1B}^{n2}}+\frac{1}{2r_{1B}^{n3}}\frac{d\varphi_{AB}^{n}(r_{1B}^{n})}{dr_{1B}^{m}}+$$

$$+\frac{3}{16r_{2B}^{n}}\frac{d^3\varphi_{AB}^{n}(r_{2B}^{n})}{dr_{2B}^{n3}}-\frac{3}{16r_{2B}^{n2}}\frac{d^2\varphi_{AB}^{n}(r_{2B}^{n})}{dr_{2B}^{n2}}+\frac{3}{16r_{2B}^{n3}}\frac{d\varphi_{AB}^{n}(r_{2B}^{n})}{dr_{2B}^{n}},\quad (36)$$

$$u_{0A_1}^{n}=u_{0A}^{n}+\frac{5}{2}\varphi_{A_1B}^{n}\left(r_{1A_1}^{n}\right),\quad (37)$$

$$k_{A_1}^{n}=k_{A}^{n}+\frac{1}{2}\sum_{i}\left[\left(\frac{\partial^2\varphi_{A_1B}^{n}}{\partial u_{i\beta}^{n2}}\right)_{eq}\right]_{r=r_{1A_1}}=k_{A}^{n}+\frac{d^2\varphi_{A_1B}^{n}\left(r_{1A_1}^{n}\right)}{dr_{1A_1}^{n2}}+\frac{3}{2r_{1A_1}^{n}}\frac{d\varphi_{A_1B}^{n}\left(r_{1A_1}^{n}\right)}{dr_{1A_1}^{n}},\quad (38)$$

$$\gamma_{1A_1}^{n}=\gamma_{1A}^{n}+\frac{1}{48}\sum_{i}\left[\left(\frac{\partial^4\varphi_{A_1B}^{n}}{\partial u_{i\beta}^{n4}}\right)_{eq}\right]_{r=r_{1A_1}}=$$

$$=\gamma_{1A}^{n}+\frac{1}{24}\frac{d^4\varphi_{A_1B}^{n}\left(r_{1A_1}^{n}\right)}{dr_{1A_1}^{n4}}-\frac{1}{6r_{1A_1}^{n}}\frac{d^3\varphi_{A_1B}^{n}\left(r_{1A_1}^{n}\right)}{dr_{1A_1}^{n3}}+\frac{11}{16r_{1A_1}^{n2}}\frac{d^2\varphi_{A_1B}^{n}\left(r_{1A_1}^{n}\right)}{dr_{1A_1}^{n2}}-\frac{11}{16r_{1A_1}^{n3}}\frac{d\varphi_{A_1B}^{n}\left(r_{1A_1}^{n}\right)}{dr_{1A_1}^{n}},\quad (39)$$

$$\gamma_{2A_1}^{n}=\gamma_{2A}^{n}+\frac{6}{48}\sum_{i}\left[\left(\frac{\partial^4\varphi_{A_1B}^{n}}{\partial u_{i\alpha}^{n2}\partial u_{i\beta}^{n2}}\right)_{eq}\right]_{r=r_{1A_1}}=\gamma_{2A}^{n}+\frac{1}{4r_{1A_1}^{n}}\frac{d^3\varphi_{A_1B}^{n}(r_{1A_1}^{n})}{dr_{1A_1}^{n3}}-$$

$$-\frac{1}{8r_{1A_1}^{n2}}\frac{d^2\varphi_{A_1B}^{n}(r_{1A_1}^{n})}{dr_{1A_1}^{n2}}+\frac{1}{8r_{1A_1}^{n3}}\frac{d\varphi_{A_1B}^{n}(r_{1A_1}^{n})}{dr_{1A_1}^{n}},\quad (40)$$

$$u_{0A_2}^{n}=u_{0A}^{n}+\frac{11}{2}\varphi_{A_2B}^{n}\left(r_{1A_2}^{n}\right),\quad (41)$$

$$k_{A_2}^{n}=k_{A}^{n}+\frac{1}{2}\sum_{i}\left[\left(\frac{\partial^2\varphi_{A_2B}^{n}}{\partial u_{i\beta}^{n2}}\right)_{eq}\right]_{r=r_{1A_2}}=k_{A}^{n}+2\frac{d^2\varphi_{A_2B}^{n}\left(r_{1A_2}^{n}\right)}{dr_{1A_2}^{n2}}+\frac{7}{2r_{1A_2}^{n}}\frac{d\varphi_{A_2B}^{n}\left(r_{1A_2}^{n}\right)}{dr_{1A_2}^{n}},\quad (42)$$

$$\gamma_{1A_2}^{n}=\gamma_{1A}^{n}+\frac{1}{48}\sum_{i}\left[\left(\frac{\partial^4\varphi_{A_2B}^{n}}{\partial u_{i\beta}^{n4}}\right)_{eq}\right]_{r=r_{1A_2}}=\gamma_{1A}^{n}+\frac{1}{24}\frac{d^4\varphi_{A_2B}^{n}(r_{1A_2}^{n})}{dr_{1A_2}^{n4}}+\frac{5}{12r_{1A_2}^{n}}\frac{d^3\varphi_{A_2B}^{n}(r_{1A_2}^{n})}{dr_{1A_2}^{n3}}+$$

$$-\frac{3}{16r_{1A_2}^{n2}}\frac{d^2\varphi_{A_2B}^{n}(r_{1A_2}^{n})}{dr_{1A_2}^{n2}}+\frac{3}{16r_{1A_2}^{n3}}\frac{d\varphi_{A_2B}^{n}(r_{1A_2}^{n})}{dr_{1A_2}^{n1}},\quad (43)$$

$$\gamma_{2A_2}^{n}=\gamma_{2A}^{n}+\frac{6}{48}\sum_{i}\left[\left(\frac{\partial^4\varphi_{A_2B}^{n}}{\partial u_{i\alpha}^{n2}\partial u_{i\beta}^{n2}}\right)_{eq}\right]_{r=r_{1A_2}}=\gamma_{2A}^{n}+\frac{1}{8}\frac{d^4\varphi_{A_2B}^{n}(r_{1A_2}^{n})}{dr_{1A_2}^{n4}}+$$

$$+\frac{3}{16r_{1A_2}^{n}}\frac{d^3\varphi_{A_2B}^{n}(r_{1A_2}^{n})}{dr_{1A_2}^{n3}}+\frac{7}{16r_{1A_2}^{n2}}\frac{d^2\varphi_{A_2B}^{n}(r_{1A_2}^{n})}{dr_{1A_2}^{n2}}-\frac{7}{16r_{1A_2}^{n3}}\frac{d\varphi_{A_2B}^{n}(r_{1A_2}^{n})}{dr_{1A_2}^{n}},\quad (44)$$

$$u_{0A}^{n}=4\varphi_{AA}^{n}\left(r_{1A}^{n}\right)+3\varphi_{AA}^{n}\left(r_{2A}^{n}\right),\ r_{2A}^{n}=\frac{2}{\sqrt{3}}r_{1A}^{n},\quad (45)$$

$$k_{A}^{n}=\frac{4}{3}\frac{d^2\varphi_{AA}^{n}\left(r_{1A}^{n}\right)}{dr_{1A}^{n2}}+\frac{8}{3r_{1A}^{n}}\frac{d\varphi_{AA}^{n}\left(r_{1A}^{n}\right)}{dr_{1A}^{n}}+\frac{d^2\varphi_{AA}^{n}\left(r_{2A}^{n}\right)}{dr_{2A}^{n2}}+\frac{2}{r_{2A}^{n}}\frac{d\varphi_{AA}^{n}\left(r_{2A}^{n}\right)}{dr_{2A}^{n}},\quad (46)$$

$$\gamma_{1A}^{n}=\frac{1}{54}\frac{d^4\varphi_{AA}^{n}\left(r_{1A}^{n}\right)}{dr_{1A}^{n4}}+\frac{2}{9r_{1A}^{n}}\frac{d^3\varphi_{AA}^{n}\left(r_{1A}^{n}\right)}{dr_{1A}^{n3}}-\frac{2}{9r_{1A}^{n2}}\frac{d^2\varphi_{AA}^{n}\left(r_{1A}^{n}\right)}{dr_{1A}^{n2}}+\frac{2}{9r_{1A}^{n3}}\frac{d\varphi_{AA}^{n}\left(r_{1A}^{n}\right)}{dr_{1A}^{n}}+$$
$$+\frac{1}{24}\frac{d^4\varphi_{AA}^{n}\left(r_{2A}^{n}\right)}{dr_{2A}^{n4}}+\frac{1}{4r_{2A}^{n2}}\frac{d^2\varphi_{AA}^{n}\left(r_{2A}^{n}\right)}{dr_{2A}^{n2}}-\frac{1}{4r_{2A}^{n3}}\frac{d\varphi_{AA}^{n}\left(r_{2A}^{n}\right)}{dr_{2A}^{n}}, \tag{47}$$

$$\gamma_{2A}^{n}=\frac{1}{9}\frac{d^4\varphi_{AA}^{n}\left(r_{1A}^{n}\right)}{dr_{1A}^{n4}}+\frac{2}{3r_{1A}^{n2}}\frac{d^2\varphi_{AA}^{n}\left(r_{1A}^{n}\right)}{dr_{1A}^{n2}}-\frac{2}{3r_{1A}^{n3}}\frac{d\varphi_{AA}^{n}\left(r_{1A}^{n}\right)}{dr_{1A}^{n}}+\frac{1}{2r_{2A}^{n}}\frac{d^3\varphi_{AA}^{n}\left(r_{2A}^{n}\right)}{dr_{2A}^{n3}}, \tag{48}$$

where φ^{m} is the interaction potential between two atoms belonging to the layer *m* (*m* is inner, next outer and outer), $r_{1X}^{m}=r_{01X}^{m}+y_{X}^{m}(T)$ is the nearest neighbor distance between the atom X and another atom belonging to the layer *m* at temperature *T*, r_{01X}^{m} is the nearest neighbor distance between the atom X and another atom belonging to the layer *m* at zero temperature and is determined from the minimum condition of the cohesive energy u_{0X}^{m}, $y_{X}^{m}(T)$ is the displacement of the X belonging to the layer *m* from the equilibrium position at temperature *T*, n_i the number of atoms on the *i*th coordination sphere, $u_{0A}^{t}, k_{A}^{t}, \gamma_{1A}^{t}, \gamma_{2A}^{t}$ are corresponding quantities of the layer *m* in the BCC pure metal in the approximation of two coordination spheres. For all atoms and layers,

$$\gamma=4\left(\gamma_1+\gamma_2\right). \tag{49}$$

The nearest neighbor distance $r_{1X}(P,0)$ between two atoms X at pressure *P* and zero temperature in all three layers satisfies the following equation of state [14], [21]

$$Pv_X=-r_{1X}\left(\frac{1}{6}\frac{\partial u_{0X}}{\partial r_{1X}}+\frac{\hbar\omega_{0X}}{4k_X}\frac{\partial k_X}{\partial r_{1X}}\right). \tag{50}$$

where $v_X=\frac{4r_{1X}^{3}}{3\sqrt{3}}$ for the BCC lattice, $\theta=k_{Bo}T, k_{Bo}$ is the Boltzmann constant, $x_X=\frac{\hbar\omega_X}{2\theta}=\frac{\hbar}{2\theta}\sqrt{\frac{k_X}{m_X}}, m_X$ is the mass of the atom X, and $\hbar=\frac{h}{2\pi}, h$ is the Planck constant. We can use Eq. (50) to determine $r_{1X}(P,0)$, the crystal parameters $k_X(P,0), \gamma_{1X}(P,0), \gamma_{2X}(P,0), \gamma_X(P,0)$ and the displacement $y_X(P,T)$. For the layer ℓ(ℓ is inner or next outer) and the outer layer [14], [21],

$$y_X^{\ell}(P,T)=\sqrt{\frac{2\gamma_X^{\ell}(P,0)\theta^2}{3\left(k_X^{\ell}\right)^3}A_X^{\ell}(P,T)},\ A_X^{\ell}(P,T)=a_{1X}^{\ell}+\sum_{i=2}^{6}\left(\frac{\gamma_X^{\ell}\theta}{\left(k_X^{\ell}\right)^2}\right)^{i}a_{iX}^{\ell}, \tag{51}$$

$$y_X^{n}(P,T)=-\frac{\gamma_X^{n}\theta}{\left(k_X^{n}\right)^2}Y_X^{n},\quad Y_X^{n}\equiv x_X^{n}\coth x_X^{n}, \tag{52}$$

where $a_{iX}^{\ell}\,(i=1\div 6)$ have the form as in [14], [21].

The nearest neighbor distances and the mean nearest neighbor distance in the layer *m* are equal to [14], [21]

$$r_{1C}^{m}(P,T)=r_{1C}^{m}(P,0)+y_{A_1}^{m}(P,T), r_{1A}^{m}(P,T)=r_{1A}^{m}(P,0)+y_{A}^{m}(P,T),$$
$$r_{1A_1}^{m}(P,T)=r_{1C}^{m}(P,T),\ r_{1A_2}^{m}(P,T)=r_{1A_2}^{m}(P,0)+y_{C}^{m}(P,T). \tag{53}$$

$$\overline{r_{1A}^{m}(P,T)}=\overline{r_{1A}^{m}(P,0)}+\overline{y^{m}(P,T)}, \overline{r_{1A}^{m}(P,0)}=\left(1-c_{B}^{m}\right)r_{1A}^{m}(P,0)+c_{B}r_{1A}'^{m}(P,0),$$
$$r_{1A}'^{m}(P,0)=\sqrt{2}r_{1C}^{m}(P,0), \overline{y^{m}(P,T)}=\sum_{X}c_{X}^{m}y_{X}^{m}(P,T), \tag{54}$$

where $c_{A}^{m}=1-7c_{B}^{m}, c_{A_1}^{m}=2c_{B}^{m}, c_{A_2}^{m}=4c_{B}^{m}, c_{X}^{m}=\dfrac{N_{X}^{m}}{N^{m}}$ is the concentration of the atom X in layer *m*, N_{X}^{m} is the number of the atom X in layer *m*, and N^{m} is the number of atoms in the layer *m*.

The Helmholtz free energy for the layer ℓ and the outer layer of the alloy film is given by [14], [21]

$$\Psi^{\ell}=N^{\ell}\left(\sum_{X}c_{X}^{\ell}\psi_{X}^{\ell}-TS_{c}^{\ell}\right),$$
$$\Psi_{X}^{\ell}=N^{\ell}\psi_{X}^{\ell}\approx U_{0X}^{\ell}+3N^{\ell}\theta[x_{X}^{\ell}+\ln(1-e^{-2x_{X}^{\ell}})]$$
$$+\frac{3N^{\ell}\theta^{2}}{\left(k_{X}^{\ell}\right)^{2}}\left[\gamma_{2X}^{\ell}\left(Y_{X}^{\ell}\right)^{2}-\frac{2\gamma_{1X}^{\ell}}{3}\left(1+\frac{Y_{X}^{\ell}}{2}\right)\right]+$$
$$+\frac{6N^{\ell}\theta^{3}}{\left(k_{X}^{\ell}\right)^{4}}\left[\frac{4}{3}\left(\gamma_{2X}^{\ell}\right)^{2}\left(1+\frac{Y_{X}^{\ell}}{2}\right)Y_{X}^{\ell}-2\left(\left(\gamma_{1X}^{\ell}\right)^{2}+2\gamma_{1X}^{\ell}\gamma_{2X}^{\ell}\right)\left(1+\frac{Y_{X}^{\ell}}{2}\right)\left(1+Y_{X}^{\ell}\right)\right], \tag{55}$$

$$\Psi^{n}=N^{n}\left(\sum_{X}c_{X}^{n}\psi_{X}^{n}-TS_{c}^{n}\right),$$
$$\Psi_{X}^{n}=N^{n}\psi_{X}^{n}\approx U_{0}^{n}+3N^{n}\theta[x_{X}^{n}+\ln(1-e^{-2x_{X}^{n}})], \tag{56}$$

where $U_{0X}^{m}=\dfrac{N^{m}}{2}u_{0X}^{m}, N^{m}$ is the number of atoms of layer *m*, u_{0X}^{m} is the cohesive energy of the atom X belonging to layer *m*, ψ_{X}^{m} is the Helmholtz free energy of atom X belonging to the layer *m* and S_{c}^{m} is the configurational entropy of the alloy in the layer *m*.

The Helmholtz free energy of the film per atom is given by

$$\frac{\Psi}{N}=\left(1-\frac{4}{n^{*}}\right)\psi^{t}+\frac{2}{n^{*}}\psi^{sn}+\frac{2}{n^{*}}\psi^{n}-\frac{TS_{c}}{N}, \tag{57}$$

where ψ^{m} is the Helmholtz free energies per atom of the layer *m*, $N=N^{t}+N^{sn}+N^{n}$ is the the total number of atoms of the film, N^{m} is the number of atoms of the layer *m*, S_{c} is the configurational entropy of the film and $n^{*}=\dfrac{N}{N^{L}}$, N^{L} is the number of atoms per layer or

$$\frac{\Psi}{N}=\frac{d\sqrt{3}-3\bar{a}}{d\sqrt{3}+\bar{a}}\psi^{t}+\frac{2\bar{a}}{d\sqrt{3}+\bar{a}}\psi^{n}+\frac{2\bar{a}}{d\sqrt{3}+\bar{a}}\psi^{sn}-\frac{TS_{c}}{N}=$$
$$=\frac{d\sqrt{3}-3\bar{a}}{d\sqrt{3}+\bar{a}}\left(\sum_{X}c_{X}^{t}\psi_{X}^{t}-TS_{c}^{t}\right)+\frac{2\bar{a}}{d\sqrt{3}+\bar{a}}\left(\sum_{X}c_{X}^{n}\psi_{X}^{n}-TS_{c}^{n}\right)+$$
$$+\frac{2\bar{a}}{d\sqrt{3}+\bar{a}}\left(\sum_{X}c_{X}^{sn}\psi_{X}^{sn}-TS_{c}^{sn}\right)-\frac{TS_{c}}{N},$$
$$d=2b^{n}+2b^{sn}+\left(n^{*}-4\right)b^{t}=\left(n^{*}-1\right)\bar{b}=\left(n^{*}-1\right)\frac{\bar{a}}{\sqrt{3}},b^{m}=\frac{a^{m}}{\sqrt{3}},a^{m}\equiv\overline{r_{1A}^{m}(P,T)},\tag{58}$$

where d is the film thickness, $\bar{a}$ is the mean nearest neighbor distance between two atoms, $\bar{b}$ is the mean thickness of two corresponding film layers, and a^{m} is the mean nearest neighbor distance in layer m.

The isothermal compressibility and elastic modulus, the thermal expansion coefficient, the heat capacity at constant volume, and the heat capacity at constant pressure of the film respectively have the form

$$\chi_{T}=\frac{3\left(\frac{\bar{a}}{\bar{a}_{0}}\right)^{3}}{2P+\frac{(\bar{a})^{2}}{3V}\left[\frac{d\sqrt{3}-3\bar{a}}{d\sqrt{3}+\bar{a}}\left(\frac{\partial^{2}\Psi^{t}}{\partial a^{t2}}\right)_{T}+\frac{2\bar{a}}{d\sqrt{3}+\tilde{a}}\left(\frac{\partial^{2}\Psi^{n}}{\partial a^{n2}}\right)_{T}+\frac{2\bar{a}}{d\sqrt{3}+\bar{a}}\left(\frac{\partial^{2}\Psi^{sn}}{\partial a^{sn2}}\right)_{T}\right]},B_{T}=\frac{1}{\chi_{T}},$$
$$\left(\frac{\partial^{2}\psi^{m}}{\partial a^{m2}}\right)_{T}=\frac{1}{N^{m}}\sum_{X}c_{X}^{m}\left(\frac{\partial^{2}\Psi^{m}}{\partial a^{m2}}\right)_{T}=\frac{1}{N^{m}}\sum_{X}c_{X}^{m}3N_{X}^{m}\left\{\frac{1}{6}\frac{\partial^{2}u_{0X}^{m}}{\partial a_{X}^{m2}}+\frac{\hbar\omega_{X}^{m}}{4k_{X}^{m}}\left[\frac{\partial^{2}k_{X}^{m}}{\partial a_{X}^{m2}}-\frac{1}{2k_{X}^{m}}\left(\frac{\partial k_{X}^{m}}{\partial a_{X}^{m}}\right)^{2}\right]\right\}.\tag{59}$$

$$\alpha=-\frac{k_{\mathrm{Bo}}\chi_{T}}{3}\left(\frac{\bar{a}_{0}}{\bar{a}}\right)^{2}\frac{\bar{a}}{3V}\left[\frac{d\sqrt{3}-3\bar{a}}{d\sqrt{3}+\bar{a}}\left(\frac{\partial^{2}\Psi^{t}}{\partial\theta\partial a^{t}}\right)_{T}+\frac{2\bar{a}}{d\sqrt{3}+\bar{a}}\left(\frac{\partial^{2}\Psi^{n}}{\partial\theta\partial a^{n}}\right)_{T}+\frac{2\bar{a}}{d\sqrt{3}+\bar{a}}\left(\frac{\partial^{2}\Psi^{sn}}{\partial\theta\partial a^{sn}}\right)_{T}\right],$$
$$\frac{1}{3N^{\ell}}\frac{\partial^{2}\Psi^{\ell}}{\partial\theta\partial a^{\ell}}=\sum_{X}c_{X}^{\ell}\left\{\frac{1}{2k_{X}^{\ell}}\frac{\partial k_{X}^{\ell}}{\partial a_{X}^{\ell}}\left(Z_{X}^{\ell}\right)^{2}+\frac{2\theta}{\left(k_{X}^{\ell}\right)^{2}}\left[\frac{\gamma_{1X}^{\ell}}{3k_{X}^{\ell}}\frac{\partial k_{X}^{\ell}}{\partial a_{X}^{\ell}}\left(2+Y_{X}^{\ell}\left(Z_{X}^{\ell}\right)^{2}\right)-\right.\right.$$
$$\left.\left.-\frac{1}{6}\frac{\partial\gamma_{1X}^{\ell}}{\partial a_{X}^{\ell}}\left(4+Y_{X}^{\ell}+\left(Z_{X}^{\ell}\right)^{2}\right)-\left(\frac{2\gamma_{2X}^{\ell}}{k_{X}^{\ell}}\frac{\partial k_{X}^{\ell}}{\partial a_{X}^{\ell}}-\frac{\partial\gamma_{2X}^{\ell}}{\partial a_{X}^{\ell}}\right)Y_{X}^{\ell}\left(Z_{X}^{\ell}\right)^{2}\right]\right\},Z_{X}^{\ell}\equiv\frac{x_{X}^{\ell}}{\sinh x_{X}^{\ell}},$$
$$\frac{1}{3N^{n}}\frac{\partial^{2}\Psi^{n}}{\partial\theta\partial a^{n}}=\sum_{X}\frac{c_{X}^{n}}{2k_{X}^{n}}\frac{\partial k_{X}^{n}}{\partial a_{X}^{n}}\left(Z_{X}^{n}\right)^{2},Z_{X}^{n}\equiv\frac{x_{X}^{n}}{\sinh x_{X}^{n}}.\tag{60}$$

$$C_{V}=\frac{d\sqrt{3}-3\bar{a}}{d\sqrt{3}+\bar{a}}C_{V}^{t}+\frac{2\bar{a}}{d\sqrt{3}+\bar{a}}C_{V}^{n}+\frac{2\bar{a}}{d\sqrt{3}+\bar{a}}C_{V}^{sn},$$
$$C_{V}^{\ell}=\sum_{X}c_{X}^{\ell}C_{XV}^{\ell}=3k_{Bo}N^{\ell}\sum_{X}c_{X}^{\ell}\left\{\left(Z_{X}^{\ell}\right)^{2}+\right.$$
$$\left.+\frac{2\theta}{\left(k_{X}^{\ell}\right)^{2}}\left[\left(2\gamma_{2X}^{\ell}+\frac{\gamma_{1X}^{\ell}}{3}\right)Y_{X}^{\ell}\left(Z_{X}^{\ell}\right)^{2}+\frac{\gamma_{1X}^{\ell}}{3}\left(1+\left(Z_{X}^{\ell}\right)^{2}\right)-\left(\left(Z_{X}^{\dagger}\right)^{4}+\left(Y_{X}^{\ell}\right)^{2}\left(Z_{X}^{\ell}\right)^{2}\right)\right]\right\},$$
$$C_{V}^{n}=\sum_{X}c_{X}^{n}C_{XV}^{n}=3k_{Bo}N^{n}\sum_{X}c_{X}^{n}\left(Z_{X}^{n}\right)^{2}.\tag{61}$$

$$C_P = C_V + 9TV\alpha^2 B_T. \tag{62}$$

At $c_B = 0$, thermodynamic quantities of alloy AB's film are equivalent to those of the main metal A's film. At a sufficiently large thickness of the thin film, thermodynamic quantities of the alloy AB's film converge to those of the bulk alloy AB.

We apply the above theory to WSi using the Mie-Lennard-Jones potential and the following approximation

$$\varphi(r) = \frac{D}{n-m}\left[m\left(\frac{r_0}{r}\right)^n - n\left(\frac{r_0}{r}\right)^m\right], \tag{63}$$

$$\varphi_{\text{W-Si}} \approx \frac{1}{2}\left(\varphi_{\text{W-W}} + \varphi_{\text{Si-Si}}\right). \tag{64}$$

Here, D is the depth of the potential well corresponding to the minimum distance r_0, m and n are numbers determined empirically through experimental fitting. The potential parameters are given in Table 1. The Mie-Lennard-Jones n-m potential is a pairwise interaction potential. In our SMM calculation results, this approach can be effectively applied to metals, substitution alloys, and interstitial alloys, where many-particle interactions contribute insignificantly.

Table 1. The Mie-Lennard-Jones potential parameters for interactions W-W and Si-Si [26]

Interaction	***m***	***n***	***D*** **(10^{-16} erg)**	**r_0 (10^{-10} m)**
W-W	6.5	10.5	15564.744	2.7365
Si-Si	6.0	12.0	45128.34	2.295

Our SMM numerical results for thermodynamic quantities of film WSi are illustrated in figures from Figure 1 to Figure 10.

Figure 1 and Figure 2 show the dependencies of the mean nearest neighbor distance ($\bar{a}$) on thickness (d), interstitial atom concentration (c_{Si}), and temperature (T) for films W and WSi. For film Wsi, at the same d and c_{Si} $\bar{a}$ increases linearly with T. For example for film W at n^* = 10 when T increases from 200 to 2000 K, $\bar{a}$ increases from 2.6643×10^{-10} m to 2.7045×10^{-10} m. For film Wsi, at the same d and T when c_{Si} increases, $\bar{a}$ also increases. For example, for film WSi at n^* = 10 and T = 300 K when c_{Si} increases from 1% to 5%, $\bar{a}$ increases from 2.6744×10^{-10}m to 2.707×10^{-10} m. For film Wsi, at the same T and c_{Si} when n^* increases, $\bar{a}$ increases slightly. For example, for film Wsi, at T = 300 K and c_{Si} = 5 % when n^* increases from 10 to 200 layers, $\bar{a}$ increases from 2.707×10^{-10} m to 2.7132×10^{-10} m.

Figure 3 shows the dependencies of the mean nearest neighbor distance $\bar{a}$ on film thickness and interstitial atom concentration for film WSi at T = 300 K. $\bar{a}$ increases with thickness and rises sharply at $d < 20$ nm. When d reaches approximately 40 nm, $\bar{a}$ of the film approaches $\bar{a}$ of the bulk material.

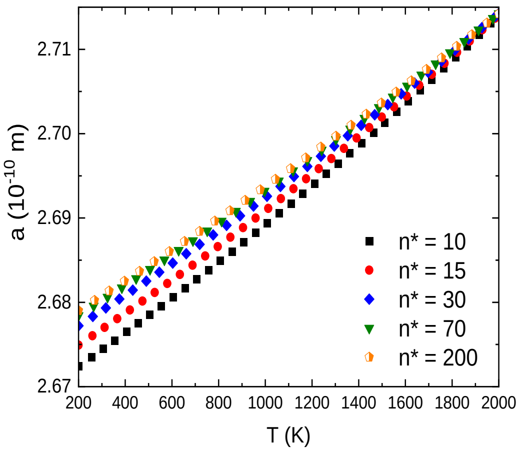

Figure 1. ***$\bar{a}$ (T, n^*) for film W calculated by SMM***

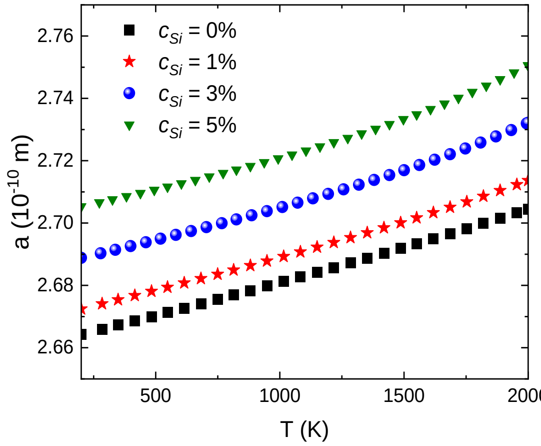

Figure 2. ***$\bar{a}$ (T, n^*) for film WSi with n^* = 10 calculated by SMM***

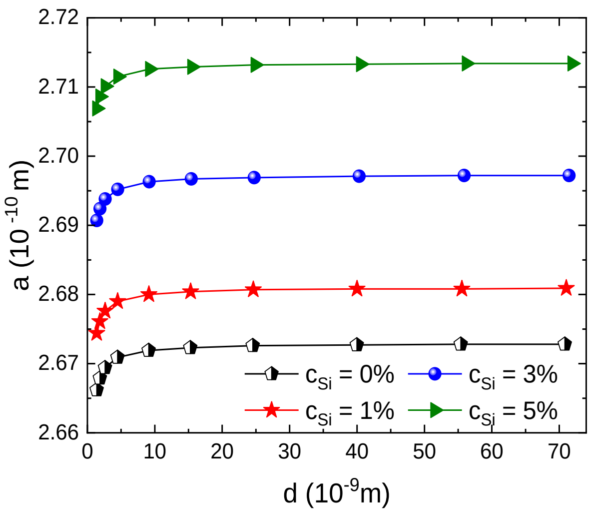

Figure 3. ***$\bar{a}$ (d, c_{Si}) for film WSi at T = 300 K calculated by SMM***

Figure 4 and Figure 5 show the thickness, interstitial atom concentration, and temperature dependences of the thermal expansion coefficient α of films W and WSi. For film Wsi, at the same d and c_{Si}, α increases nonlinearly as T increases. For example, for film WSi at $n^* = 10$ and $c_{Si} = 5$ % when T increases from 200 to 2000 K, α increases from 0.6305×10^{-5} K^{-1} to 0.8068×10^{-5} K^{-1}. For film Wsi, at the same d and T when c_{Si} increases, α increases. For example, for film WSi at n^* =10 and T = 2000 K when c_{Si} increases from zero to 5%, α increases from 2.7045×10^{-5} K^{-1} to 2.7502×10^{-5} K^{-1}. For film Wsi, at the same T and c_{Si} when n^* increases, α decreases. For example film.

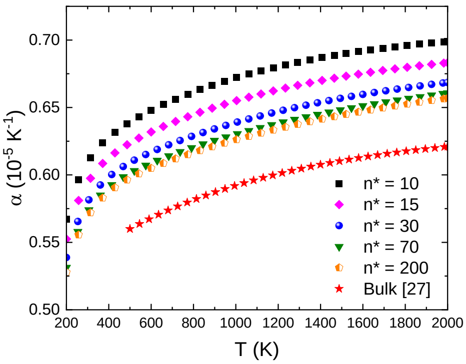

Figure 4.** $\alpha(T, n^*)$ **for film W calculated by SMM

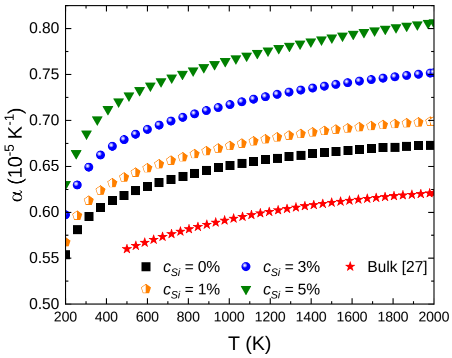

Figure 5.** $\alpha(T, c_{Si})$ **for film WSi with** n^* **= 10 calculated by SMM

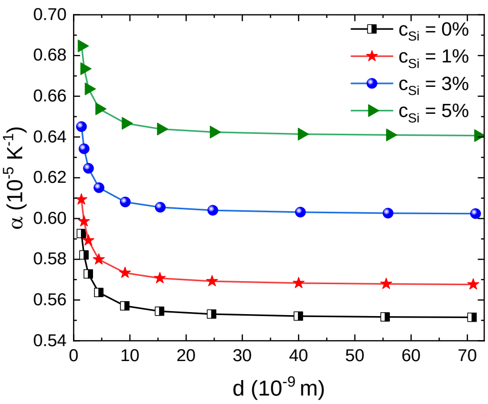

Figure 6.** $\alpha(d, c_{Si})$ **for film WSi at** T **= 300 K calculated by SMM

WSi at T = 2000 K and c_{Si} = 5 % when n^* increases from 10 to 200 layers, α decreases from 2.7502×10^{-5} K^{-1} to 2.7462×10^{-5} K^{-1}. These results are in good agreement with available results [12], [27]

Figure 6 shows the film thickness and interstitial atom concentration dependences of the thermal expansion coefficient α for film WSi at T = 300 K. α decreases as d increases. That is also consistent with the rule of metal film.

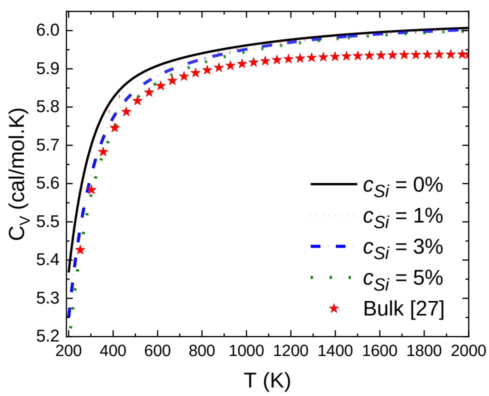

Figure 7.** C_V (T, c_{Si}) **for film WSi with** n^* **= 10 calculated by SMM

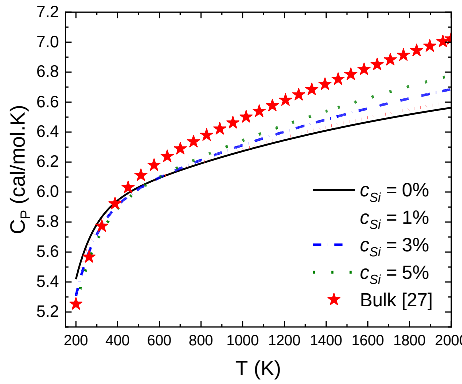

Figure 8.** C_P (T, c_{Si}) **for film WSi with** n^* **= 10 calculated by SMM

Figure 7 and Figure 8 show interstitial atom concentration and temperature dependences of heat capacities at constant volume and constant pressure C_V, C_P of films W and WSi with n^* =10. For film Wsi, at the same thickness d and c_{Si} when T increases, C_V and C_P increase nonlinearly. For example, for film WSi at n^* = 10 and c_{Si} = 5% when T increases from 200 to 2000 K, C_V and C_P increase from 5.1716 cal/mol.K to 6.0013 cal/mol.K and from 5.2317 cal/mol.K to 6.7792 cal/mol.K. For film WSi at the same d and T when c_{Si} increases, C_V decreases and C_P increases. For example for film WSi at n^* = 10 and T = 2000 K when c_{Si} increases from zero to 5 %, C_V and C_P decrease slightly from 6.0089 cal/mol.K to 6.0013 cal/mol.K and increase from 6.5031 cal/mol.K to 6.7792 cal/mol.K. When T increases, the C_V of the film increases sharply in the low temperature region and decreases slightly in the high temperature region, whereas C_P increases sharply in the high temperature region. This is explained by the fact that the contribution of the anharmonic effect increases as T increases. On the other hand, it shows that C_V decreases as c_{Si} increases, while C_P increases as c_{Si} increases. The temperature and concentration dependencies of C_V and C_P have the same rules for bulk metals and metal films [21].

To confirm the reliability of our SMM calculation results, we present the currently available data on bulk W. The temperature dependence of mean nearest neighbor distance and some thermodynamic quantities for bulk W at zero pressure from available data sources is shown in Table 2.

Table 2. Temperature dependence of mean nearest neighbor distance and some thermodynamic quantities for bulk W at zero pressure from available data sources

T(K)	200	500	800	1500	2000
$\bar{a}\left(\mathrm{\mathring{A}}\right)$ [28]	2.6482	2.6537	2.6572	2.6680	2.6758
$\chi_T\left(10^{-12}\mathrm{Pa}\right)$ [28]	1.824	1.698	1.756	1.990	2.2143
$\alpha\left(10^{-5}\mathrm{K}^{-1}\right)$ [29], [30]	0.41	0.46	0.48	0.56	0.64
	0.560	0.571	0.578	0.602	0.621
$C_V\left(\mathrm{cal/mol.K}\right)$ [28]	5.15	5.81	5.89	5.93	5.94
$C_P\left(\mathrm{cal/mol.K}\right)$ [29], [30]	-	6.09	6.34	6.91	7.33
	5.253	6.101	6.357	6.777	7.021

Figure 9 and Figure 10 show interstitial atom concentration and film thickness dependences of C_V and C_P of films W and WSi at T = 300 K. When d < 20 nm, the C_V and C_P of the film decrease quite sharply. When d increases to about 40 nm, the C_V and C_P of the film approach the values of bulk materials [21], [27]. Conversely, C_V and C_P decrease as c_{Si} increases. This behavior of the heat capacities, both at constant volume and constant pressure, in relation to the thickness and concentration of interstitial atoms can be explained as follows: As the thickness increases (and consequently the number of layers), the mean nearest neighbor increases initially increases rapidly within the thickness range from 0 to 10 nm and then gradually slows, eventually approaching the value typical of the bulk material at around 40 nm thickness. Therefore, both C_V and C_P decrease sharply within the 0 to 10 nm thickness and then decrease more gradually, approaching the values of the bulk material at about 40 nm thickness. Similarly, as the concentration of interstitial atoms increases, leading to an increase in the mean nearest neighbor also increases. C_V and C_P consequently decrease, in agreement with the values of the bulk material at about 40 nm thickness.

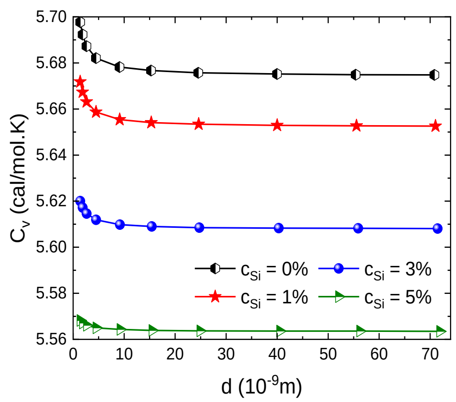

***Figure 9.** C_V (d, c_{Si}) for films W and WSi at T = 300 K calculated by SMM*

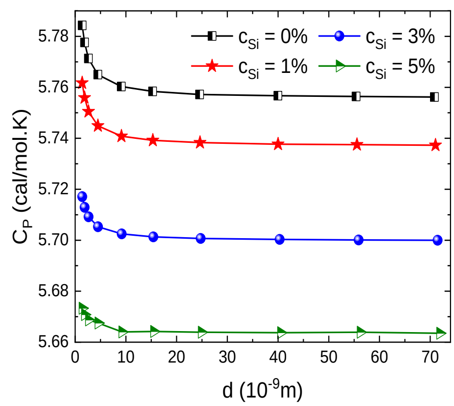

***Figure 10.** C_P (d, c_{Si}) for films W and WSi at T = 300 K calculated by SMM*

3. Conclusions

The article introduces a model and a novel thermodynamic theory that includes analytical expressions for Helmholtz free energy, crystal parameters for the film's layers, the mean nearest neighbor distance, and various thermodynamic quantities as functions of temperature, concentration of interstitial atoms, and film thickness for BCC interstitial binary alloy's film, based on the SMM framework. Notably, the crystal parameters for the outer layer and the next outer layer are newly developed contributions. The theoretical framework is employed in numerical calculations for W and WSi alloy utilizing the Mie-Lennard-Jones potential and the coordination sphere method. The SMM numerical results for films W and WSi are compared with those for bulk W and WSi. The SMM numerical results for film WSi are compared with those for film W. The SMM numerical results for the thermal expansion coefficient and the heat capacity at constant pressure of bulk W are in good agreement with experimental data. It is observed that the mean nearest neighbor distance increases with temperature, interstitial atom concentration, and the number of layers. Likewise, the thermal expansion coefficient increases with temperature, and interstitial atom concentration and decreases with an increasing number of layers. Similarly, the heat capacity at constant pressure increases with temperature, and interstitial atom concentration and decreases with film thickness. We recommend experimental investigations into the dependencies of the thermodynamic quantities on film thickness and interstitial atom concentration for metal (W) and interstitial alloy (WSi), as delineated by our SMM analyses. In a subsequent article, we plan to explore the pressure dependence of thermodynamic quantities for W and Wsi films using the SMM.

REFERENCES

[1] Liang LH & B. Li B, (2006). Size-dependent thermal conductivity of nanoscale semiconducting systems. *Physical Review B*, 73(15),153303.

[2] Kolska Z, Ziha J, Hnatowicz V & Svorcik V, (2010). Lattice parameter and expected density of Au nano-structures sputtered on glass. *Materials Letters*, 64, 1160-1162

[3] Liang LH, Li JC & Jiang Q, (2002). Size-dependent elastic modulus of Cu and Au thin films. *Solid State Communications*, 121(8), 453-455.

[4] Nakao S, Ando T, Shikida M & Sato K, (2006). Mechanical properties of micronsizes SCS film in a high temperature environment. *Journal of Micromechanics and Microengineering*, 16, 715.

[5] Chen S, Liu L & Wang T, (2005). Investigation of the mechanical properties of thin films by nanoindentation considering the effects of thickness and different coating-substrate combinations. *Surface & Coatings Technology*, 191, 25-32.

[6] Huntz AM, Marechal L, Lesage B & Molins M, (2006). Thermal expansion coefficient of alumina films developed by oxidation of a FeCrAl alloy determined by a deflection technique. *Applied Surface Science*, 252, 7781-7787.

[7] Cornella G, Lee S, Kraft O, Nix WD & Bravman JC, (1998). Determination of temperature dependent untressed lattice spacings in crystalline thin films on substrates. *MRS Online Proceedings Library*, 505, 527-532.

[8] Forrest JA, Dalnoki-Veress K, Steven JR & Dutcher JR, (1996). Effect of free surfaces on the glass transition temperature of thin polymer films. *Physical Review Letters*, 77(10)2002.

[9] Zoo Y, Adams D, Mayer JW & Alford TL, (2006). Investigation of coefficient of thermal expansion of silver thin film on different substrates using X-ray diffraction. *Thin Solid Films*, 513, 170-174.

[10] Kraft O & Nix WD, (1998). Measurement of the lattice thermal expansion coefficients of thin metal films on substrates. *Journal of Applied Physics*, l.83, 3035-3038.

[11] Fuks D, Dorfman S, Zhukovskii F, Kotomin A & Stoneham AM, (2001). Theory of the growth mode for a thin metallic film on an insulating substrate. *Surface Science*, 499, 24-40.

[12] Fang W & Lo CY, (2000). On the thermal expansion coefficients of thin films. *Sensors and Actuators*, 84, 310-314.

[13] Bui TT & Dao VD, (2010). Measurement of mechanical and thermal properties of co-sputtered WSi thin film for MEMS applications. *Microsystem Technologies*, 16, 1881-1886.

[14] Nguyen TH, Nguyen QH & Hua XD, (2023). Study on the thermodynamic properties of a thin film of FCC interstitial alloy AuSi at zero pressure using the statistical moment method. *Physics*, 5, 59-68.

[15] Nguyen T & Vu VH, (1998). Investigation of the thermodynamic properties of anharmonic crystals by the momentum method. I. General results for face-centred cubic crystals. *Physica Status Solidi (b),* 149(2), 511-519.

[16] Vu VH & Masuda- Jindo K, (2000). Application of statistical moment method to thermodynamic properties of metals at high pressures. *Journal of the Physical Society of Japan*, 69, 2067.

[17] Nguyen QH, Bui DT & Nguyen DH, (2020). Stress-strain curve of FCC interstitial alloy WSi under pressure. *Romanian Journal of Physics,* 65(608), 1-12.

[18] Nguyen QH, Nguyen DH, Nguyen NL, Vu TL, Pham HT & Le HV, (2021). Study on the diffusion of interstitial atoms in interstitial alloy WSi with BCC structure. *HNUE Journal of Science, Natural Sciences*, 66(1), 30-41.

[19] Nguyen QH, Nguyen DH, Nguyen MH & Vu QT, (2021). Combining the Mie-Lennard-Jones and the Morse potentials in studying the elastic deformation of interstitial alloy AgC with FCC structure under pressure. *VNU Journal of Sciences: Mathematics-Physics*, 37(2), 31-42.

[20] Nguyen QH, Nguyen DH, Nguyen TH, Nguyen NL & Le LH, (2022). Study on diffusion in metals Si, Cu and interstitial alloys WSi, CuSi with BCC structure under pressure. *HNUE Journal of Science, Natural Sciences*, 67(1), 27-37

[21] Nguyen QH, Hua XD & Pham TT, (2023). Thermodynamic and elastic properties of tungsten and tungsten silicide. *Modern Physics Letters B*, 37, 2350006.

[22] Duong DP, Vu VH & Nguyen TH, (2013). The coefficients of thermal expansion of thin metal films were investigated using the statistical moment method. *Journal of Science of HNUE,* 58(7),109-116.

[23] Vu VH, Duong DP & Nguyen TH, (2013). Investigation of thermodynamic properties of metal thin film by statistical moment method. *Communications in Physics*, 23(4), 301-311.

[24] Vu VH, Duong DP & Nguyen TH, (2014). Thermodynamic properties of free standing thin metal films: Temperature and pressure dependences. *Communications in Physics,* 24(2), 177-191.

[25] Vu VH, Duong DP, Nguyen TH & Ho KH, (2015). Theoretical investigation of the thermodynamic properties of metallic thin films. *Thin Solid Films,* 583, 7-12.

[26] Magomedov MN, (2006). The calculation of the parameters of the mie-lennard-jones potential. *High Temperature,* 44(4), 513-529.

[27] Gray DE, (1972). *American Institute of Physics Handbook.* 3rd Edition McGraw-Hill, Tx.

[28] Vu VH, Nguyen TH & Nguyen QB, (1997). Investigation of the thermo-dynamic properties of anharmonic crystals with defects by the moment method. *Journal of the Physical Society of Japan*, 66, 3494-3498.

[29] Billings BH et al., (1963). *American Institute of Physics Handbook*, New York: McGraw-Hill Book Company.

[30] Vu VH, (2009). *Statistical moment method in studying elastic and thermodynamic properties of the crystal*. University of Education Publisher, p. 131.